

Entanglement in spin network states

Based on works 2204.03093 and 2205.11205

Qian Chen

Laboratoire de Physique, ENS de Lyon

06/12/2022

Overview

- 1 Introduction
- 2 Curvature from multipartite entanglement
- 3 Entanglement coarse-graining
- 4 Conclusion

Table of Contents

- 1 Introduction
- 2 Curvature from multipartite entanglement
- 3 Entanglement coarse-graining
- 4 Conclusion

Loop quantum gravity

Canonical loop quantum gravity (LQG) quantizes GR *à la* topological quantum field theory / lattice quantum field theory:

- Starting point: connection-triad field variables [Ashtekar, 1986]

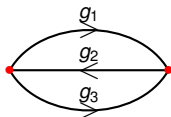
$$\{A_a^i(x), E_j^b(y)\} = \delta_j^i \delta_a^b \delta(x, y),$$

$$\underbrace{\text{Gaussian + spatial diffeo. constraints}}_{\text{kinematics}} + \underbrace{\text{Hamiltonian constraint}}_{\text{dynamics}} .$$

- The wave-function of LQG state is based on (closed) oriented graph

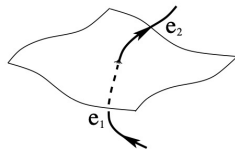
$$\psi_\Gamma(\{g_e\}_{e \in \Gamma}) = \psi_\Gamma(g_1, g_2, \dots),$$

$g_e \in \text{SU}(2)$ holonomy (exponentiating A_a^i): parallel transport matrix.



Holonomy-flux algebra and intertwiner

- Holonomy-flux algebra:
 $[E_i, g] = g_2 \tau_i g_1$,
 where τ_i is $\mathfrak{su}(2)$ Lie algebra basis,
 and $g = g_2 g_1$.



- Fourier decomposition to $SU(2)$ -function (Peter-Weyl)

$$\psi(g_e) = \sum f_{m_e n_e}^{j_e} D_{m_e n_e}^{j_e}(g_e), \quad g_e \text{—position, } j_e \in \frac{\mathbb{N}}{2} \text{—momentum}$$

- Assign intertwiner tensor ι_v to each vertex v , in order to make wave-function gauge-invariant under $g_e \rightarrow h_{t(e)} g_e h_{s(e)}^{-1}$

$$\iota_v : \bigotimes_{e \ni v} \mathcal{V}_{j_e} \rightarrow \bigotimes_{e' \ni v} \mathcal{V}_{j_{e'}}.$$

- Intertwiner recouples spins into zero-angular momentum state (singlet), entangling edge states naturally.

Spin networks

A spin network basis state consists of triple data $(\Gamma, \{j_e\}, \{l_v\})$.

- The wave-function of spin network basis state is glued by holonomies and intertwiners,

$$\Psi_{\{j_e, l_v\}}(\{g_e\}_{e \in \Gamma}) = \sum_{m_e^{t,s}} \prod_e \sqrt{2j_e + 1} \langle j_e m_e^t | g_e | j_e m_e^s \rangle \prod_v \langle \bigotimes_{e|v=s(e)} j_e m_e^s | l_v | \bigotimes_{e|v=t(e)} j_e m_e^t \rangle.$$

- Diffeomorphism invariance:



Advances and challenges

LQG took a big step forwards:

- Non-perturbative approach avoids divergence.
- Background independence: No referring to fixed background space-time.
- Admit quantum superposition and fluctuation of spin network states.

As well as some challenges and **prescription**:

- The problem of locality: How do we localize subsystems in the sense of diffeomorphism invariance? → **relational perspective** [Rovelli,1996] (emerging from relation between subsystems.)
- Semi-classical limit: How do we recover classical general relativity from the quantum theory? → **coarse-graining** [Dittrich, 2012], [Bodendorfer,2021].
- Dynamics: Hamiltonian is complicated. → **holography: the conserved charges of d-dim region can be defined on the (d-1)-dim boundary** [Freidel, Geiller, Pranzetti, 2020].

QIT becomes relevant for LQG

Quantum information theory is crucial for loop quantum gravity. Without background geometry, quantum geometry/gravity should be reconstructed from quantum information.

- Black hole, information paradox [Rovelli, 1996], [Ashtekar, et al, 1998], [Perez, 2017], [Bianchi, Haggard, 2018].
- Area law [Freidel, Livine, 2010], volume law [Bianchi et al, 2022].
- Decoherence [Feller, Livine, 2017], [Fahn, Giesel, Kobler, 2022].
- Tensor network perspective [Chirco, Oriti, Zhang, 2018], [Colafranceschi, Chirco, Oriti, 2022].
- Typicality and thermal space-time [Anzà, Chirco, 2017], [Chirco, Kotecha, Oriti, 2019].
- Quantum reference frame [Carrozza, Höhn, 2021].
- Quantum simulation of quantum gravity [Cohen et al, 2021].

Dynamics and holography

Quantum gravity's dynamics is holographic, inspired by, for instance

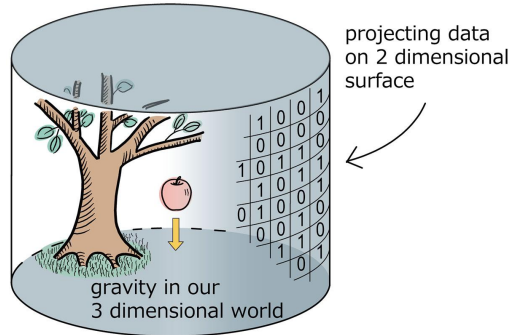
- Black hole entropy: $S = \frac{1}{4}A$.
- Quasi-local conserved charges: e.g., Brown-York energy [Brown, York, 1993], [Yang, Ma, 2009], [Odak, Speziale, 2021]

$$E_{quasi-local} = \int_{\partial\Sigma} (2d \text{ extrinsic curvature}) dS$$

Holographic principle:

Gravitational degrees of freedom in d -dim manifold can be encoded on the $d - 1$ -dim boundary.

In this talk, we put bulk-boundary relation into emphasis!



The goals of this talk

Entanglement: the unfactorizability of quantum states [the correlations that can't be interpreted classically] → Composite quantum state carries more information than all its local states.

Dictionary between quantum geometry and correlations (in LQG):

- Distance [[Feller, Livine, 2016](#)].
- Metric [[Baytas, Bianchi, Yokomizo, 2018](#)].
- Curvature? See later.

I simply outline the goals of this talk:

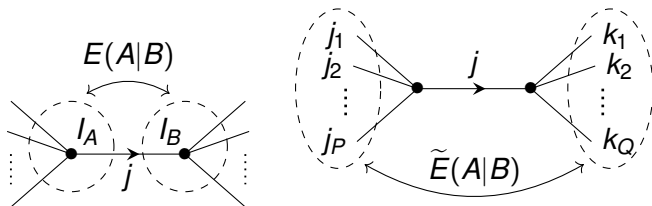
- To study entanglement in spin network states: multipartite entanglement measure.
- To reconstruct the gauge curvature from the notion of quantum entanglement and correlations.
- To see how bulk-boundary relation makes sense in the context of entanglement.

Table of Contents

- 1 Introduction
- 2 Curvature from multipartite entanglement**
- 3 Entanglement coarse-graining
- 4 Conclusion

Intertwiner entanglement v.s. boundary entanglement

Simplest case: single-link graph [Livine, 2018]



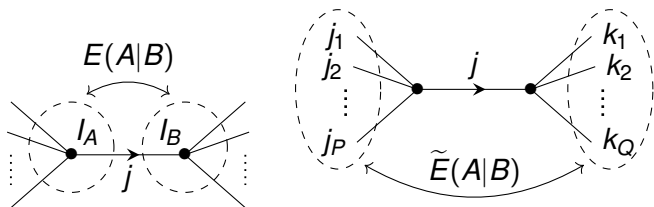
- Intertwiner entanglement $E(A|B)$: with respect to $\mathcal{H}_A \otimes \mathcal{H}_B$,

$$\mathcal{H}_A = \text{Inv} \left(\bigotimes_{e \ni A} \mathcal{V}_{j_e} \otimes \mathcal{V}_j \right), \quad \mathcal{H}_B = \text{Inv} \left(\bigotimes_{e \ni B} \mathcal{V}_{j_e} \otimes \mathcal{V}_j \right).$$

- Boundary entanglement $\tilde{E}(A|B)$: with respect to $\mathcal{H}_A^\partial \otimes \mathcal{H}_B^\partial$,

$$\mathcal{H}_A^\partial = \bigotimes_{e \ni A} \mathcal{V}_{j_e}, \quad \mathcal{H}_B^\partial = \bigotimes_{e \ni B} \mathcal{V}_{j_e}.$$

Intertwiner entanglement v.s. boundary entanglement



Basic features of intertwiner entanglement:

- Spin network basis state: $E(A|B) = 0$.
- Entanglement emanates from spin-superpositions and intertwiner-correlations.

Basic features of boundary entanglement:

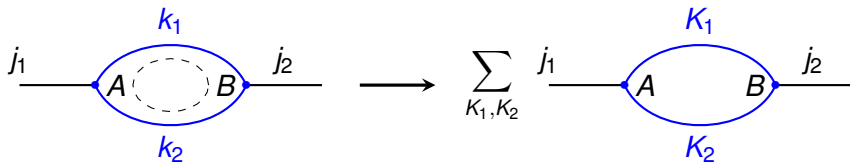
- Spin network basis state: $\tilde{E}(A|B) = \ln(2j + 1)$.
- The entanglement doesn't depend on the holonomy inserted. This can be confirmed by gauge transformation.

Entanglement excitation

We focus on intertwiner entanglement, which is defined by the unfactorizability between

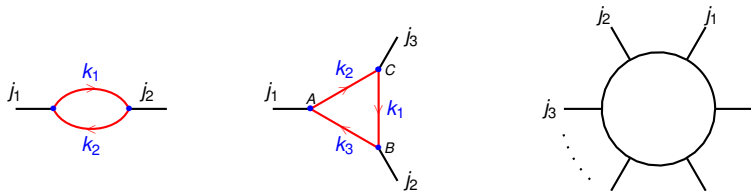
$$\mathcal{H}_\Gamma \subset \bigotimes_{v \in \Gamma} \mathcal{H}_v .$$

Consider a spin network basis state (with fixed spins) as initial state, which does not carry any intertwiner entanglement. After implementing a loop holonomy operator, intertwiner entanglement is created since the operator introduces spin-superposition. For instance, on candy graph:



Entanglement excitation

I focus on trivalent spin network with one topological loop¹ in the sense of $L = E^o - V + 1$ where E^o and V are numbers of bulk edges and vertices, respectively. The curvature gets reflected in loop holonomy operator.



¹We will explain this when comes to gauge-fixing. In fact, we can compute the entanglement from boundary, by using the method in the next part.

Loop holonomy operator

The loop holonomy acts on spin network state in the following way:

- Loop holonomy operator χ_ℓ associated to loop W is defined by

$$\chi_\ell(\mathbf{g}_W) = \sum_{m_i} D_{m_1 m_2}^\ell(\mathbf{g}_1) D_{m_2 m_3}^\ell(\mathbf{g}_2) \cdots D_{m_n m_1}^\ell(\mathbf{g}_n),$$

where ℓ is the spin of SU(2) representation, and $\chi_\ell(\mathbf{g}) = \text{Tr}[D^\ell(\mathbf{g})]$.

- The operator $\hat{\chi}_\ell$ acts on spin network ψ_Γ by multiplication

$$\hat{\chi}_\ell(\mathbf{g}_W) \triangleright |\psi_\Gamma(\mathbf{g})\rangle = \chi_\ell(\mathbf{g}_W) |\psi_\Gamma(\mathbf{g})\rangle.$$

The representation of loop holonomy operator

- Each D^ℓ introduces a spin-superposition along piecewise edge:

$$D^\ell \otimes D^k = \bigotimes_{|k-\ell|}^{k+\ell} D^{k'}$$

Then loop holonomy operator is represented by a product of series of $6j$ -symbols.

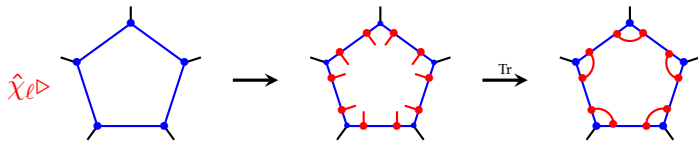


Figure: The graphical representations for loop holonomy operator χ_ℓ .

Representation of holonomy operator

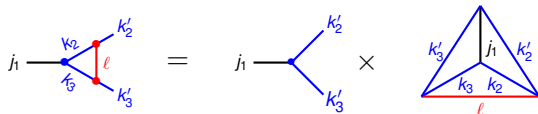
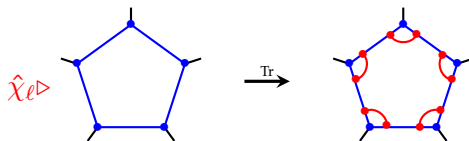


Figure: Each corner brings a $6j$ -symbol to the representation of holonomy operator.



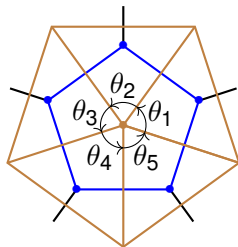
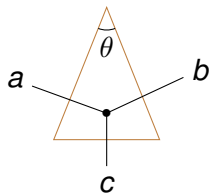
Finally,

$$\begin{aligned}
 [Z_{\ell}^{\{j_i\}}]^{\{K_i\}}_{\{k_i\}} &= \int \prod_{e \in \Gamma} dg_e \overline{\Psi_{\{j_i, K_i\}}(\{g_e\}_{e \in \Gamma})} \chi_{\ell}(G_W) \Psi_{\{j_i, k_i\}}(\{g_e\}_{e \in \Gamma}) \\
 &= (-1)^{\sum_{i=1}^n (j_i + k_i + K_i + \ell)} \prod_{i=1}^n \left\{ \begin{matrix} j_i & K_i & K_{i+1} \\ \ell & k_{i+1} & k_i \end{matrix} \right\} \prod_{i=1}^n \sqrt{(2K_i + 1)(2k_i + 1)}.
 \end{aligned}$$

Representation of holonomy operator: large spins limit

Via asymptotic 6j-symbol when $\ell \ll c, a, b$ and $\cos \theta = \frac{a(a+1)+b(b+1)-c(c+1)}{2\sqrt{a(a+1)b(b+1)}}$

$$\left\{ \begin{matrix} c & a & b \\ \ell & b + \varepsilon_2 & a + \varepsilon_1 \end{matrix} \right\} \approx \frac{(-1)^{a+b+c+\ell+\varepsilon_2}}{\sqrt{(2a+1)(2b+1)}} d_{\varepsilon_2 \varepsilon_1}^{\ell}(\theta).$$



The asymptotic Z is expressed in terms of angles θ_i , and spin-shiftings ε_i ,

$$[Z_{\ell}^{\{j_i\}}]^{\{K_i\}}_{\{k_i\}} \approx \prod_{i=1}^n d_{\varepsilon_i \varepsilon_{i+1}}^{\ell}(\theta_i), \quad \text{with } \varepsilon_i = K_i - k_i.$$

Multipartite entanglement

Multipartite entanglement has richer structure than bipartite entanglement.

- Schmidt form $|\psi_{AB}\rangle = (U_A \otimes U_B) \sum_{i=1}^d \sqrt{\lambda_i} |i_A\rangle \otimes |i_B\rangle$ can not be generalized in general, i.e., generically,

$$|\psi_{ABC}\rangle \neq (U_A \otimes U_B \otimes U_C) \sum_{i=1}^d \sqrt{\lambda_i} |i_A\rangle \otimes |i_B\rangle \otimes |i_C\rangle.$$

- Fragile entanglement, e.g., $|GHZ\rangle = \frac{1}{\sqrt{2}}(|000\rangle + |111\rangle)$.
- Non-fragile entanglement, e.g., $|W\rangle = \frac{1}{\sqrt{3}}(|001\rangle + |010\rangle + |100\rangle)$.

Entanglement measure form multipartite entanglement

- There are many inequivalent entanglement measures for multipartite entanglement.
- We adopt geometric entanglement as entanglement measure: for a pure state ψ , it is defined by [\[Wei, Goldbart, 2003\]](#)

$$S_g[\psi] = -\ln \max_{\phi} |\langle \psi | \phi \rangle|^2,$$

where $|\phi\rangle$ takes from all product states (unentangled).

- The goal is to study the evolution of geometric entanglement:
 $S_g[\psi_0] = 0 \rightarrow S_g[\psi_t]$ where $|\psi_t\rangle = e^{-it\hat{H}}|\psi_0\rangle$.

Entanglement and dispersion

On trivalent one-loop spin network, our results about geometric entanglement excitation are listed as follows [QC, Livine, 2022]:

- The 1st- and 2nd-order derivatives of geometric entanglement are

$$\frac{dS_g[\psi_t]}{dt}\Big|_{t=0} = 0, \quad \frac{1}{2} \frac{d^2 S_g[\psi_t]}{dt^2}\Big|_{t=0} = \langle \psi_0 | \hat{H}^2 | \psi_0 \rangle - \langle \psi_0 | \hat{H} | \psi_0 \rangle^2.$$

- The general expressions match the computation on truncated state²

$$|\psi_{t(2)}\rangle := |\psi_0\rangle - it\hat{H}|\psi_0\rangle - \frac{1}{2}t^2\hat{H}^2|\psi_0\rangle,$$

that is, $S_g[\psi_{t(2)}] = (\langle \psi_0 | \hat{H}^2 | \psi_0 \rangle - \langle \psi_0 | \hat{H} | \psi_0 \rangle^2)t^2 + O(t^4)$.

²It is normalized up to fourth-order of t , i.e. $\langle \psi_{t(2)} | \psi_{t(2)} \rangle = 1 + O(t^4)$.

Entanglement and dispersion

- In particular, we can compute linear entropy $S_{lin} = 1 - \text{Tr}(\rho^2)$ by the dispersion. For instance, the bipartite linear entanglement entropy in candy graph is given by

$$S_{lin}[\rho_A(t)] = 2(\langle \psi_0 | \hat{H}^2 | \psi_0 \rangle - \langle \psi_0 | \hat{H} | \psi_0 \rangle^2) t^2 + O(t^4).$$

- In large-spin limit, using asymptotic formula for 6j-symbol as $\ell \ll c, a, b$,

$$S_g \approx \sum_{s=0}^{2\ell} \prod_{\nu} P_s(\cos \theta_{\nu}) - \prod_{\nu} P_{\ell}(\cos \theta)^2.$$

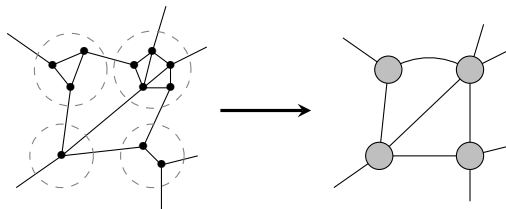
Here P_{ℓ} are Legendre polynomials.

Table of Contents

- ① Introduction
- ② Curvature from multipartite entanglement
- ③ Entanglement coarse-graining**
- ④ Conclusion

Coarse-graining

Coarse-graining:=
reduction of graphic structure,



- Tracing over bulk holonomies \longrightarrow boundary density matrix [QC, Livine, 2021].
- Gauge-fixing bulk holonomies \longrightarrow loopy spin network.

In this part, we focus on

- The 'gauge-fixing' coarse-graining approach.
- Evolution of the coarse-graining.
- The entanglement between spin sub-networks: $\mathcal{H}_\Gamma \subset \bigotimes_i \mathcal{H}_{\Gamma_i}$
(Generalization of intertwiner entanglement).

Spin network with boundary

Entanglement between sub-networks involves boundaries.

We consider a spatial region with boundary which is described by an open spin network. This picture is motivated by the study of black hole entropy.

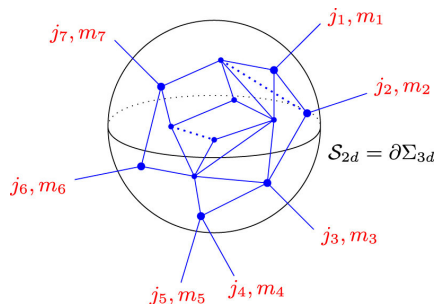


Figure: Spin network for a spatial region with 2d boundary where each 1d edge punctures the boundary and presents a dual 2d area element [Livine, 2021].

Boundary Hilbert space and bulk-boundary map

Every open edge carries $SU(2)$ representation. The boundary Hilbert space is defined as

$$\mathcal{H}_{\partial\Gamma} = \bigotimes_{e \in \partial\Gamma} \mathcal{H}_e.$$

- A spin network wave-function defines a bulk-boundary map in terms of functional [\[QC, Livine, 2021\]](#):

$$\psi_{\Gamma} : \{\mathbf{g}_{e \in \Gamma^o}\} \rightarrow \mathcal{H}_{\partial\Gamma}, \quad \{\mathbf{g}_{e \in \Gamma^o}\} \mapsto |\psi_{\partial\Gamma}(\{\mathbf{g}_{e \in \Gamma^o}\})\rangle.$$

- Under gauge transformation $\mathbf{g}_e \mapsto h_{t(e)} \mathbf{g}_e h_{s(e)}^{-1}$:

$$|\psi_{\partial\Gamma}(\{h_{t(e)} \mathbf{g}_e h_{s(e)}^{-1}\}_{e \in \Gamma^o})\rangle = \left(\bigotimes_{e \in \partial\Gamma} h_{v(e)}^{\epsilon_v} \right) |\psi_{\partial\Gamma}(\{\mathbf{g}_e\}_{e \in \Gamma^o})\rangle,$$

- Bulk-boundary maps make up a dual Hilbert space $(\mathcal{H}_{\partial})^*$, with the same scalar product as spin networks: for any $|\phi_{\partial\Gamma}\rangle, |\psi_{\partial\Gamma}\rangle \in (\mathcal{H}_{\partial})^*$,

$$\langle \phi_{\partial\Gamma} | \psi_{\partial\Gamma} \rangle := \int \prod_{e \in \Gamma^o} d\mathbf{g}_e \langle \phi_{\partial\Gamma}(\{\mathbf{g}_{e \in \Gamma^o}\}) | \psi_{\partial\Gamma}(\{\mathbf{g}_{e \in \Gamma^o}\}) \rangle.$$

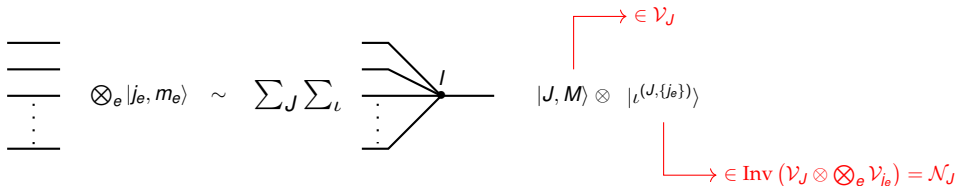
Tensor product decomposition

$|\psi_{\partial\Gamma}(\{\mathbf{g}_{e \in \Gamma^o}\})\rangle$ is a boundary state associated with the bulk-boundary map ψ_Γ .

- Any $|\psi_{\partial\Gamma}(\{\mathbf{g}_{e \in \Gamma^o}\})\rangle$ admits a decomposition $\bigotimes_e \mathcal{V}_{j_e} = \bigoplus_J \mathcal{V}_J \otimes \mathcal{N}_J$:

$$|\psi_{\partial\Gamma}(\{\mathbf{g}_{e \in \Gamma^o}\})\rangle \in \mathcal{H}_{\partial\Gamma} = \bigoplus_{\{j_e\}} \bigotimes_{e \in \partial\Gamma} \mathbb{C}|j_e, m_e\rangle = \bigoplus_{\{j_e\}} \bigoplus_{J, M} \mathbb{C}|J, M\rangle \otimes |\iota^{(J, \{j_e\})}\rangle,$$

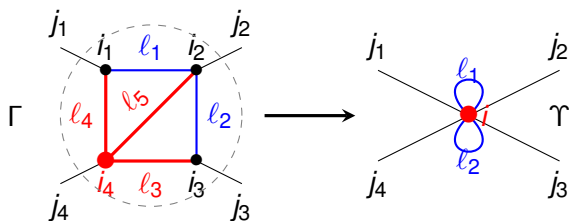
- Total spin $J \in \mathbb{N}$ due to the gauge invariance of spin network state.
- Intertwiner $\iota^{(J, \{j_e\})}$ encodes the recoupling $\{j_e\} \rightarrow J$.



Coarse-graining via gauge-fixing

The 'gauge-fixing' coarse-graining procedure — $\Gamma \rightarrow \Upsilon$ [Freidel, Livine, 2003]:

- Choose a 'root vertex' (in red) and a 'maximal tree' in bulk (in red): connect all vertices by a path that doesn't form a loop.
- Implement gauge transformation $g_e \rightarrow h_t g_e h_s^{-1}$ along the maximal tree to set these holonomies $g_e \mapsto 1$.
- Contract along the maximal tree. Edges out of the maximal tree become self-loops (in blue). Thus we obtain a loopy spin network.



Coarse-graining via gauge-fixing

Gauging-fixing from $|\psi_{\partial\Gamma}\rangle$ to $|\psi_{\partial\Upsilon}\rangle$,

$$|\psi_{\partial\Gamma}(\{\mathbf{g}_e\}_{e\in\Gamma^o})\rangle = \left(\bigotimes_{e\in\partial\Gamma} h_{v(e)}^{\epsilon_e^v} \right) |\psi_{\partial\Upsilon}(\{\mathbf{G}_e\}_{e\in\Upsilon^o})\rangle,$$

Gauge-fixing preserves the scalar product, from the viewpoint of bulk-boundary map [\[QC, 2022\]](#),

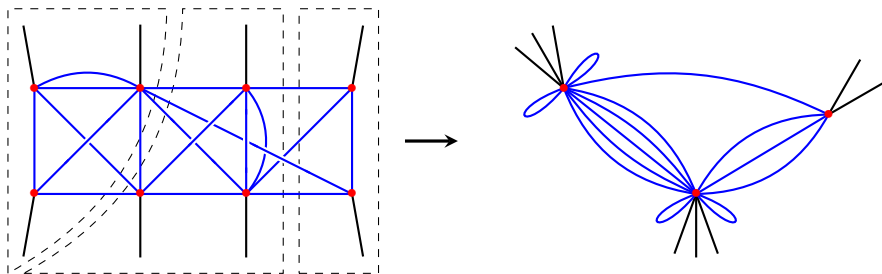
$$\langle\phi_{\partial\Gamma}|\psi_{\partial\Gamma}\rangle = \langle\phi_{\partial\Upsilon}|\psi_{\partial\Upsilon}\rangle.$$

- A local unitary transformation w.r.t. the sub-network

$$|\psi_{\partial\Gamma}\rangle = U_B |\psi_{\partial\Upsilon}\rangle, \quad U_B \in \mathcal{U}[(\mathcal{H}_\partial)^*, (\mathcal{H}_\partial)^*].$$

Entanglement coarse-graining

- Spin network entanglement is preserved under the coarse-graining.



$$E(\Gamma_1 : \Gamma_2 : \Gamma_3) = E(\Upsilon_1 : \Upsilon_2 : \Upsilon_3).$$

Loop holonomy operator and its coarse-graining

This local unitary transformation also leads to

holonomy operator transformation : fined graph \leftrightarrow coarse-grained graph

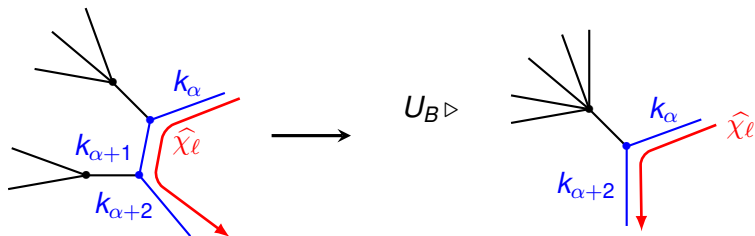
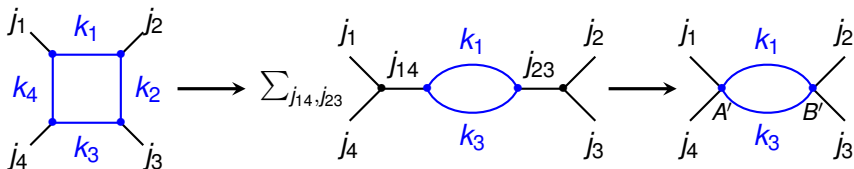


Figure: On fined graph, the data for the representation of loop holonomy operator are $\ell, k_\alpha, k_{\alpha+1}, k_{\alpha+2}$ and recoupled spins. Gauge-fix the holonomy for spin $k_{\alpha+1}$ into \mathbb{I} in the left side, then contract it.

An example: square graph to candy graph



The transformation rule is in the form of $Z_W = U_A U_B Z_L U_A^\dagger U_B^\dagger$

$$\begin{aligned}
 & (-1)^{\sum_{i=1}^4 (j_i + k_i + K_i + \ell)} \begin{Bmatrix} j_1 & k_1 & k_4 \\ \ell & K_4 & K_1 \end{Bmatrix} \begin{Bmatrix} j_2 & k_2 & k_1 \\ \ell & K_1 & K_2 \end{Bmatrix} \begin{Bmatrix} j_3 & k_3 & k_2 \\ \ell & K_2 & K_3 \end{Bmatrix} \begin{Bmatrix} j_4 & k_4 & k_3 \\ \ell & K_3 & K_4 \end{Bmatrix} \\
 = & \sum_{j_{14}} \sum_{j_{23}} (-1)^{j_{14} + j_{23} + k_1 + K_1 + k_3 + K_3 + 2\ell + 2k_2 + 2k_4 - 2K_2 - 2K_4} (2j_{14} + 1)(2j_{23} + 1) \begin{Bmatrix} j_1 & j_4 & j_{14} \\ K_3 & K_1 & K_4 \end{Bmatrix} \\
 & \times \begin{Bmatrix} j_2 & j_3 & j_{23} \\ K_3 & K_1 & K_2 \end{Bmatrix} \begin{Bmatrix} j_{14} & k_1 & k_3 \\ \ell & K_3 & K_1 \end{Bmatrix} \begin{Bmatrix} j_{23} & k_1 & k_3 \\ \ell & K_3 & K_1 \end{Bmatrix} \begin{Bmatrix} j_1 & j_4 & j_{14} \\ k_3 & k_1 & k_4 \end{Bmatrix} \begin{Bmatrix} j_2 & j_3 & j_{23} \\ k_3 & k_1 & k_2 \end{Bmatrix}.
 \end{aligned}$$

Entanglement coarse-graining: evolution of spin network

The spin network entanglement is still preserved under coarse-graining.

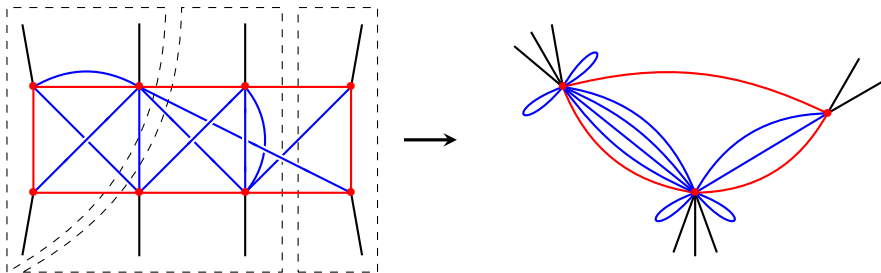


Figure: The red path is the loop on which holonomy operator acts. The evolution of spin network entanglement still gets reflected in the evolution of intertwiner entanglement between loopy vertices.

Entanglement excitation and closure defects

A direct corollary is about entanglement excitation considered in Part 2.

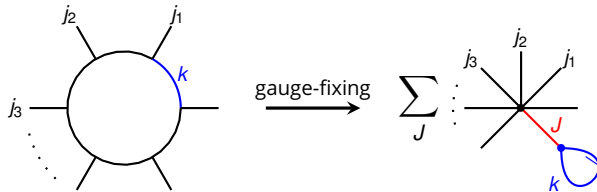


Figure: Gauge-fixing for trivalent one-loop spin network. We call W the loop on left-hand side, and L the loop on right-hand side

Then we can compute the entanglement by

$$\langle \psi_0 | \hat{\chi}_\ell(\mathbf{g}_W) | \psi_0 \rangle = \langle \tilde{\psi}_0 | \hat{\chi}_\ell(\mathbf{g}_L) | \tilde{\psi}_0 \rangle, \quad \langle \psi_0 | \hat{\chi}_\ell(\mathbf{g}_W)^2 | \psi_0 \rangle = \langle \tilde{\psi}_0 | \hat{\chi}_\ell(\mathbf{g}_L)^2 | \tilde{\psi}_0 \rangle.$$

Entanglement excitation and total spin

The computation of entanglement excitation is relevant to total spin- J and corresponding probability $p(k_J)$,

- Firstly, gauge-fixing tells us the boundary state written as

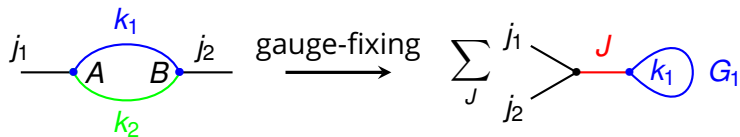
$$|\tilde{\psi}_0(\mathbf{G})\rangle_{\partial} = \sum_J e^{i\varphi_k(J)} \sqrt{p_k(J)} \sum_{a,b=-k}^k \sqrt{2k+1} (-1)^{k-a} D_{ab}^k(\mathbf{G}) \begin{pmatrix} J & k & k \\ M & b & -a \end{pmatrix} |J, M\rangle$$

- So the dispersion is given by the expectation from $|\psi_0(\mathbf{G})\rangle_{\partial}$:

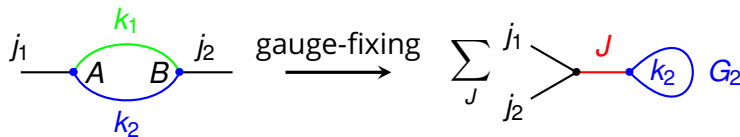
$$\begin{aligned} \frac{1}{2} \frac{d^2 S_g}{dt^2} \Big|_{t=0} &= \sum_J p_k(J) \sum_{s=0(1)}^{2\ell} (-1)^{J+s+2k} \begin{Bmatrix} J & k & k \\ s & k & k \end{Bmatrix} (2k+1) \\ &\quad - \left(\sum_J p_k(J) (-1)^{J+\ell+2k} \begin{Bmatrix} J & k & k \\ \ell & k & k \end{Bmatrix} (2k+1) \right)^2. \end{aligned}$$

Example: candy graph

The entanglement excitation can be computed from boundary state:



(a)



(b)

Figure: The gauge-fixings on candy graph. The green labels the maximal tree.

Example: candy graph

- Two paths of gauge-fixing lead to two probability distributions:

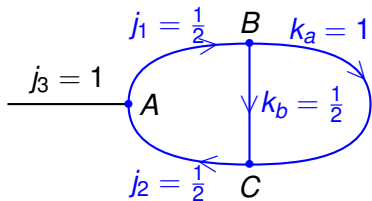
$$p_{k_1}(J) = (2k_2 + 1)(2J + 1) \left\{ \begin{matrix} J & k_1 & k_1 \\ k_2 & j_1 & j_2 \end{matrix} \right\}^2,$$

$$p_{k_2}(J) = (2k_1 + 1)(2J + 1) \left\{ \begin{matrix} J & k_2 & k_2 \\ k_1 & j_1 & j_2 \end{matrix} \right\}^2.$$

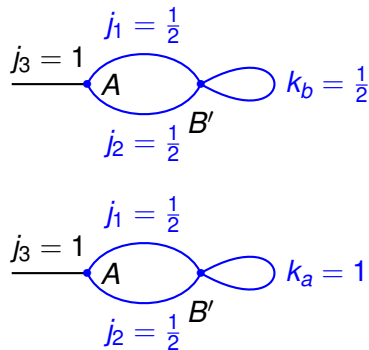
- But the entanglement excitations are same. For instance, for $p_{k_1}(J)$,

$$\begin{aligned} \frac{1}{2} \frac{d^2 S_g}{dt^2} \Big|_{t=0} &= \sum_J p_{k_1}(J) \sum_{s=0(1)}^{2\ell} (-1)^{J+s+2k_1} \left\{ \begin{matrix} J & k_1 & k_1 \\ s & k_1 & k_1 \end{matrix} \right\} (2k_1 + 1) \\ &\quad - \left(\sum_J p_{k_1}(J) (-1)^{J+\ell+2k_1} \left\{ \begin{matrix} J & k_1 & k_1 \\ \ell & k_1 & k_1 \end{matrix} \right\} (2k_1 + 1) \right)^2. \end{aligned}$$

Example: path-dependency — spin-dependency



(a) Holonomy operator acts along path $j_1 \rightarrow k_a \rightarrow j_2$ or path $j_1 \rightarrow k_b \rightarrow j_2$.



(b) The coarse-grained graphs for path choices.

The path dependency is reflected on the spin of self-loop.

$$S_{lin}(\rho_{aA}) = \frac{7t^2}{9} + O(t^3), \quad S_{lin}(\rho_{bA}) = \frac{26t^2}{27} + O(t^3).$$

Table of Contents

- ① Introduction
- ② Curvature from multipartite entanglement
- ③ Entanglement coarse-graining
- ④ Conclusion

Summary

Along the study of bulk-boundary map, we present the spin network entanglement:

- Geometric entanglement as multipartite entanglement measure for loop quantum gravity.
- 2-order entanglement excitation equals the dispersion of loop holonomy operator.
- The spin network entanglement get reflects in loopy intertwiners.
- The spin network entanglement is preserved under coarse-graining, as well as its evolution provided that the evolution is generated by holonomy operator (curvature reconstruction).
- The coarse-graining implies that the d.o.fs relevant to entanglement are encoded in boundary information and bulk topology.

Thanks for your attention!